Humping Formation in High Current GTA Welding

Patricio F. Mendez, Krista L. Niece and Thomas W. Eagar
Massachussetts Institute of Technology, Cambridge, MA

In proceedings of the International Conference on Joining of Advanced and Speciality Materials II, Cincinnati, OH, November 1999

Abstract

Welding productivity increases with welding speed and current, however this strategy is limited by the appearance of defects such as humping. In this work the generation of this defect is studied by analyzing a very depressed weld pool at high current and welding speed. Under these conditions, the front of the weld pool turns into a thin layer of liquid, and a force balance in the molten metal determine whether the thin liquid layer will transport liquid to the rear of the weld pool, or freeze prematurely producing a humped bead. The conclusions obtained permit to explain the shape of the process envelope for GTAW welding observed in experiments, and allow for the analysis of practical alternatives for its expansion.

Introduction

The increase of welding productivity has a significant economic impact, estimated in the order of several hundred million dollars in yearly worldwide savings. Humping is one of the most common defects that limit welding productivity.

Increases in welding speed have to be matched by increases in the heat input, otherwise the cross section of the weld would decrease, eventually not reaching melting at any point. The heat input into the workpiece can be calculated as

$$\text{heat input} = \eta I V \tag{1}$$

where η is the arc efficiency, I is the welding current, and V is the arc voltage.

The most practical way to increase the heat input is to increase the welding current, because the voltage and efficiency of the arc vary only moderately. The limit to a strategy of continuous increase in the welding speed and current is the appearance of defects such as humping. Humping can be defined as an irregular surface contour consisting of a series of bead-like protuberances (Figure 1).

Other defects that originate in the weld bead are tunnelling, split bead and parallel humping. Tunnelling is a defect in which an open channel, which remains unfilled with weld metal is formed at the root (Figure 2).

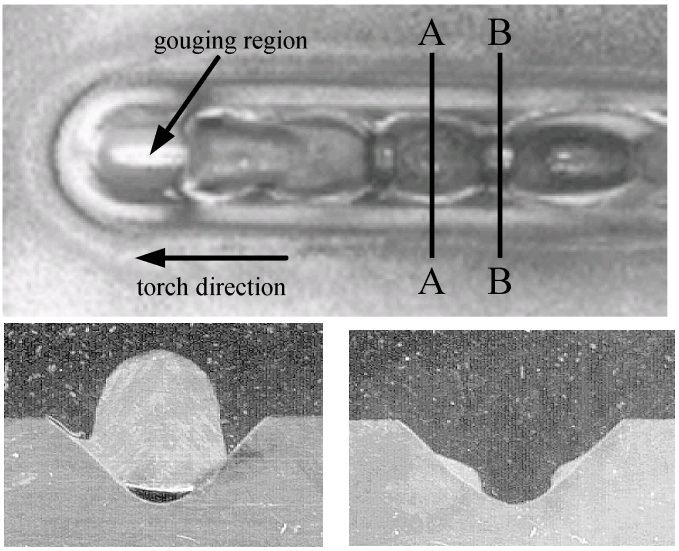

Figure 1: Humping in GTAW. The top figure is a top view of the humped weld seam, the bottom left picture is a cross section of the bead-like protuberance (cross section A-A), and the bottom right is a cross section of the void between beads (cross section B-B).

In a split bead the weld seam is split into two independent parallel seams separated by an empty channel in between, and parallel humping is a type of split bead in which the parallel seams are humped (Figure 3.

The occurrence of humping is associated with a large depression of the weld pool observed at high currents and velocities. Bradstreet[1] studied humping formation in GMAW, and associated it with the presence of an "arc crater" where the surface of the weld pool was very de-

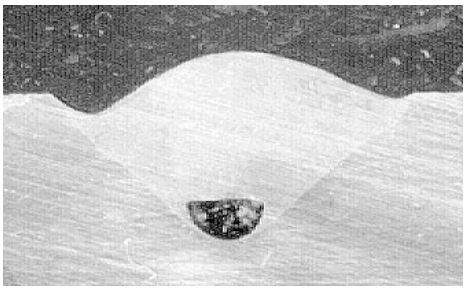

Figure 2: Tunnelling in GTAW. The cross section of the channel appears at the root of the weld.

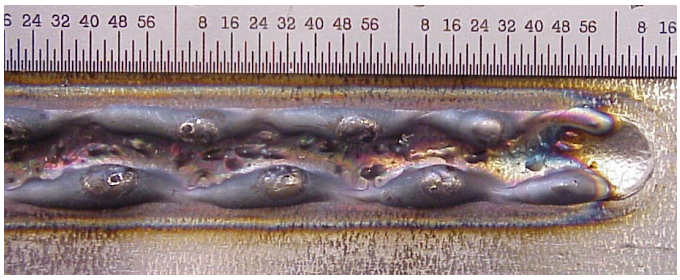

Figure 3: Parallel humping in GTAW. The two parallel humped beads can be seen on the sides of an empty groove.

pressed. He proposed capillary instability as the mechanism for humping. Yamamoto and Shimada[2, 3] performed research on GTAW at low pressure, and concluded that the onset of humping was related to a transition in which the weld pool turned into a thin film under the arc. In their theory humping would occur when molten metal velocity in the thin film exceeds the critical value for a hydraulic jump. Figure 4 shows the process map they obtained empirically. Savage *et al.* [4] determined experimentally a relationship between the presence of defects at atmospheric pressure and welding current and speed. The occurrence of defects in the weld pool depends mainly on the welding current and travel speed, as shown in the process map of Figure 5.

Some processes such as laser welding or deposition of microdroplets [5] show humping, but in these cases the liquid pool is long enough so as to generate capillary instabilities. Gratzke *et al.* [6] concluded that humping cannot be due to the Marangoni effect, as suggested by Mills and Keene [7]. Although their observation is valid, their capillary instability calculations do not apply to most arc welding situations, where the weld pool geometry is very different from an elongated cylinder.

In this paper, a mechanism for humping based on the premature freezing of the gouging region is proposed. This mechanism can explain the presence of humping in weld beads that are too short to experience a capillary instability.

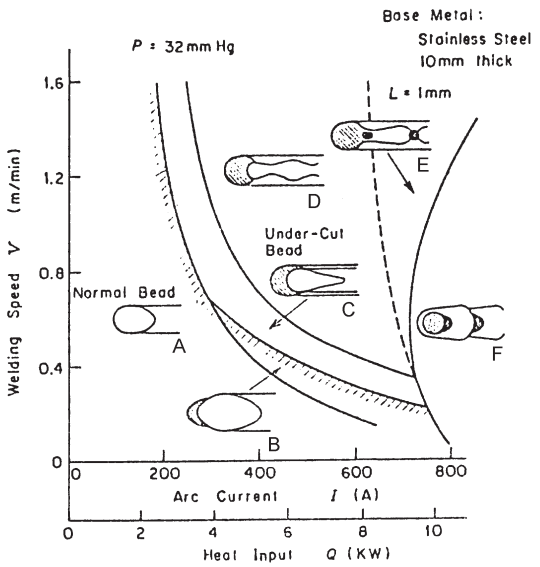

Figure 4: Process map for GTAW at 0.04 atm, after Shimada *et al.* [3]. Each region contains a particular type of weld bead. Type A is a normal weld pool, with little surface depression. Type B is a sound weld, but the front of the weld pool is being "gouged". Type C has more severe gouging and produces an undercut weld. Type D presents two parallel humped beads at the side of the welds, and a "dry" path in between them. Type E is similar to type D, but the parallel beads collapse into each other, sometimes leading to tunnelling. Type F presents "dry" spots in between humps.

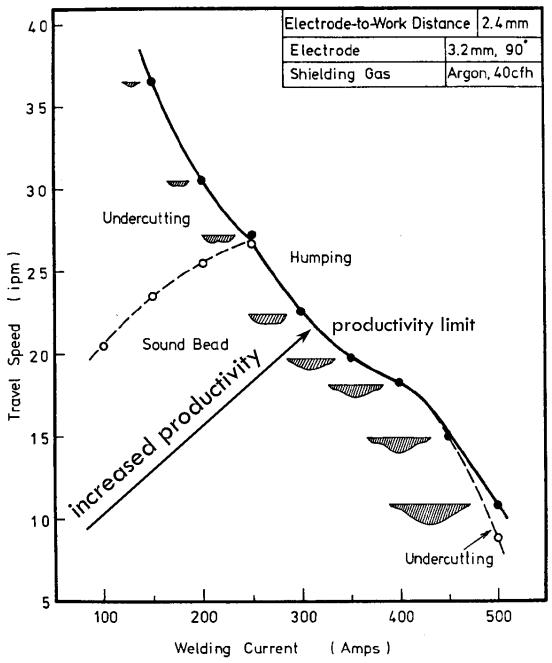

Figure 5: Process map for GTAW at atmospheric pressure, after Savage *et al.* [4]. When the travel speed or welding current are too high, defects occur.

Weld Pool Geometry At High Current and Velocity

Figure 6 shows top, cross and longitudinal views of a GTA weld produced at high current and travel speed; Figure 7 shows a schematic of a weld pool in that regime. The most salient feature is the deep depression of the free surface, exhibiting a "gouging region" under the arc, a "rim" around it, and a bulk of molten metal ("trailing region") at the rear of the weld pool. The gouging region is a very thin layer of liquid where there are no recirculating flows. The rim around the gouging region is a thicker liquid portion that transports molten metal to the trailing region at the rear of the weld pool. The transition line delimits the sharp transition between the gouging region and the trailing region. It was observed experimentally that this line moves toward the rear as the current increases[8, 3]. The elements of the weld pool present different configurations depending on the welding parameters. These variations are the origin of different defects such as humping, tunnelling, split bead, and parallel humping. It can be seen in Figure 6 that the cross section of a good weld shows no obvious signs of the very depressed surface that occurs during the melting process.

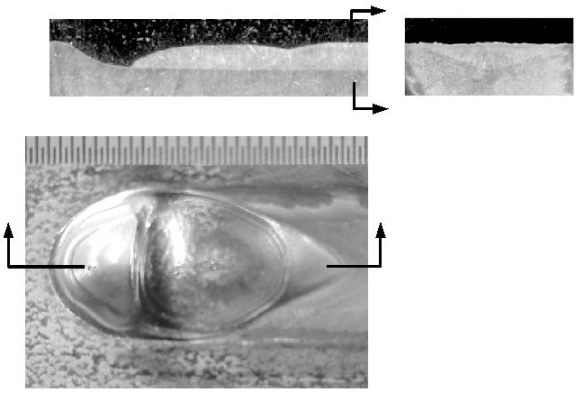

Figure 6: Weld pool at high currents and speeds (AISI 304, 500 A, 35.4 ipm)

Humping Threshold

If the gouging region extends to a point where there is not enough heating from the arc it will freeze, producing a void in the weld seam. The time scale for freezing is very short; it can be estimated by balancing the rate of heat extraction at the solid-liquid interface, and the heat capacity of the thin layer:

$$\text{time scale for freezing} = \left(\frac{1}{2}\frac{kT_C}{\alpha} + \rho\Delta H_{sl}\right)\frac{\delta_C}{Q_{max}} \qquad (2)$$

where T_C and δ_C are the characteristic temperature jump and thickness of the thin liquid film, k, α, ρ are the thermal

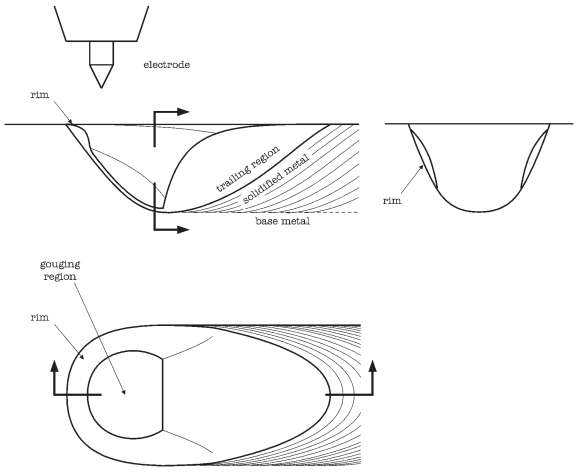

Figure 7: Schematic of the weld pool at high currents and speeds. The free surface is very depressed, turning into a thin liquid film under the arc. A thicker rim of liquid runs around the edge of the weld pool carrying molten metal to the bulk of liquid at the rear of the weld pool. The transition line marks the abrupt change from the thin liquid film into the bulk of liquid at the rear.

conductivity, thermal diffusivity, and density of the substrate, ΔH_{sl} is the latent heat of melting, and Q_{max} is the characteristic heat input from the arc. The values of T_C and δ_C can be estimated by performing an order of magnitude scaling of the gouging region [9].

$$\widehat{T}_C = Q_{max}\widehat{\delta}/k \qquad (\approx 100\,\mathrm{K})$$
$$\widehat{\delta}_C = (2\mu U_\infty D/\tau_{max})^{1/2} \qquad (\approx 50\,\mu\mathrm{m})$$

where $\widehat{T}_C$ and $\widehat{\delta}_C$ are the estimated values of T_C and δ_C. The symbols, μ, U_∞, D, and τ_{max} correspond to the viscosity of the molten metal, welding speed, welding penetration, and aerodynamic drag from the arc respectively.

A typical value for the time scale for freezing is of the order of a few milliseconds. Such fast freezing indicates that for all practical purposes, the gouging region will freeze immediately if it reaches a cold section of the metal, and the humping process will start, as shown schematically in Figure 8. The location of the transition point is therefore critical; humping will start when the transition point is pushed far enough towards the rear of the weld pool into the region where the heat from the arc is too little.

Location of the Transition Point

Forces Acting on the Transition Point

The location of the transition point is determined by a balance of the forces acting on it, as shown in Figure 9. These forces are: hydrostatic, capillary, arc pressure and shear, other forces (Marangoni, electromagnetic, etc.).

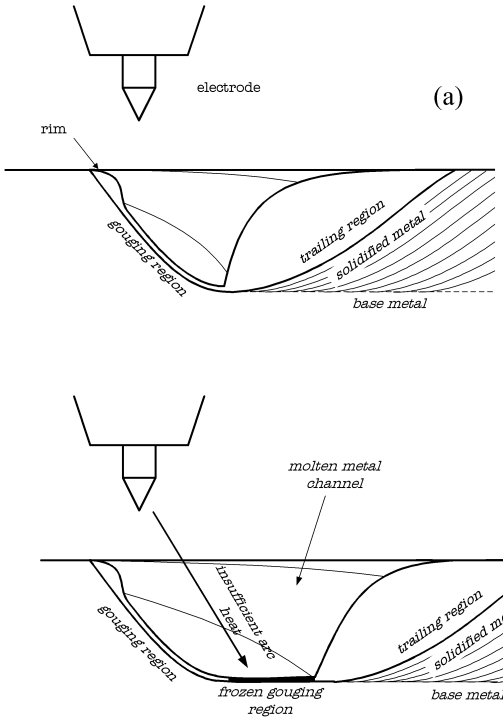

Figure 8: Schematic of humping formation in GTAW. Figure (a) illustrates a weld pool in which the gouging region does not extend far from the arc, therefore the thin liquid layer feeds the trailing region, and humping does not happen. Figure (b) represents a weld pool in which the trailing region starts far from the arc. In this case, the further portion of the trailing region does not receive enough heat from the arc and freezes almost instantly. The trailing region is fed by two molten metal channels, one on each side of the weld, surrounding the gouging region with a rim of molten metal. Figure (c) shows the evolution of the weld of Figure (b). The side channels start to solidify, and stop feeding the trailing region, which also begins to solidify. With no possibility of transferring molten metal to the rear of the weld pool a new humped bead starts to form.

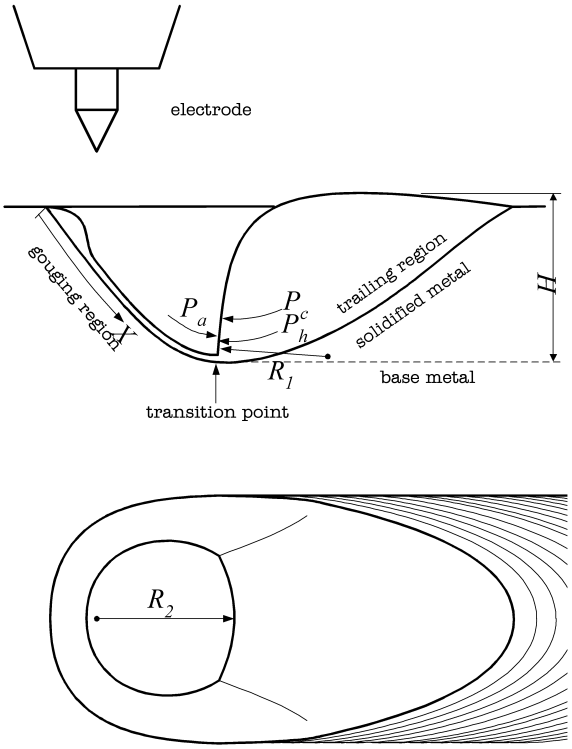

Figure 9: Forces acting at the transition point

The hydrostatic forces are originated by the pressure due to the column of metal (H in Figure 9) between the transition point and the highest point of the free surface. Their expression is:

$$P_h = \rho g H \tag{3}$$

where g is the acceleration of gravity. The expression for the capillary forces is:

$$P_c = \sigma \left(\frac{1}{R_1} + \frac{1}{R_2} \right) \tag{4}$$

where σ is the surface tension and R_1 and R_2 are the principal curvatures of the free surface at the transition point, with R_1 being the curvature on the plane of symmetry. The simple appearance of this equation is misleading, because these curvatures are very difficult to obtain or predict; they can also be positive or negative.

The arc pressure and shear are due to the impingement of the plasma on the free surface. For a flat surface the arc pressure has symmetry of revolution, with a distribution profile resembling that of a gaussian distribution. Very little is known about the behavior of a welding arc on very irregular geometries such as those encountered on very depressed weld pools in traveling welds. In those cases, the symmetry of revolution is broken, and the arc force is expected to increase with the deformation [10]. For relatively slow welds, the weld pool is located directly below the arc, and its depression resembles that of static welds. For faster welds, the distance traveled before melting starts is longer;

therefore, the weld pool shifts towards the rear of the arc. In this situation the arc force acts on the front of the weld pool, facilitating the creation of the gouging region, and pushing the transition point towards the rear.

The arc pressure and gas shear affect all of the free surface, but its influence decreases with the distance from the electrode, being negligible when the rear of the weld pool extends too far.

On the verge of humping, the transition point is at the edge of the arc with the trailing region behind; therefore, very little action from the arc on the trailing region is expected in welds on the verge of humping.

The arc pressure scales with the square of the current, therefore, at higher currents, the arc pressure will push the transition point to the rear.

Many other forces act on the trailing region, such as Marangoni, electromagnetic and buoyancy. These forces are induced by the action of the arc, which is very weak over the trailing region on the verge of humping. These forces are expected to be of little importance for influencing the onset of humping.

Force Balance at the Transition Point

The location of the transition point can be determined by a force balance. The forces involved are the arc pressure (P_a), which tends to expand the size of the gouging region, pushing the transition point to the rear, and the hydrostatic and capillary forces (P_h and P_c respectively), which push the transition point to the front, thus decreasing the size of the gouging region.

$$P_a = P_h + P_c \tag{5}$$

The force balance can be expressed in a non-dimensional form using the following scaling relationships:

$$X = X_C x \tag{6}$$
$$R_1 = H r_1 \tag{7}$$
$$R_2 = X r_2 \tag{8}$$
$$P(X) = P_{max} p(x) \tag{9}$$

In these scaling relationships the uppercase symbols correspond to magnitudes with dimensions, and the lower case symbols correspond to dimensionless magnitudes. The relationships are chosen such that the dimensionless magnitudes are approximately one. The radius R_1 is scaled with the hydrostatic head, and R_2 with the size of the gouging region. The distance X is scaled with X_C, which is the distance of influence of the arc. In an arc over a flat surface, this distance would be the arc radius, in arcs acting over a very depressed surface the arc diameter would be a better approximation. Values of x smaller than one correspond to points "inside" the arc, and values of x larger than one to points "outside" the arc, in the cold region.

The force balance at the transition point can be expressed with the following non-dimensional relationship:

$$p(x) = \frac{\sigma}{X_C P_{max}} \left[\frac{1}{r_2} + \frac{X_C}{H} \left(\frac{\rho g H^2}{\sigma} - \frac{1}{r_1 x} \right) \right] \tag{10}$$

The arc pressure $P(X)$ for flat surfaces is commonly approximated by a Gaussian distribution. The actual shape of the function differs when the weld pool presents a large depression, but no studies have been performed so far in that situation. In this study the numerical values obtained by Choo [11] for flat surfaces and experimental values quoted by Lin [12] will be used.

The expression for the maximum pressure can be correlated from Choo's numerical examples for an argon arc:

$$P_{max} = 5.616 \times 10^{-3} I^{1.956} h^{-0.216} \tag{11}$$

where P_{max} is the characteristic arc pressure measured in Pascals, I is the welding current in Ampères and h is the arc length in millimeters.

The arc radius stays approximately constant at approximately 1.9 mm for arc lengths ranging between 1 and 5 mm and currents up to 300 A, therefore X_C could be estimated as 2.8 mm.

The radius R_1 is of the order of magnitude of the depth from top of the free surface in the trailing region to the bottom of the gouging region (metallostatic head). This radius is influenced by the "contact angle" of the trailing region at the transition point. A wetting angle yields a lower curvature than a non-wetting angle. Experiments showed that 304 stainless steel with 6 ppm of sulfur has a larger wetting contact angle than with 230 ppm (Figure 10). The effect of the contact angle is not considered explicitly in the scaling relationships stated above.

The position of the transition point is determined by solving equation 10 for x. Values of x larger than one correspond to a gouging region that extends beyond the area heated by the arc, therefore humping occurs.

Stability of the Gouging Region

Equation 10 can be represented graphically as in Figure 11. The left member of equation 10 shows the normalized arc pressure, represented by p_a. In Figure 11 the arc pressure is represented as a gaussian with its center at the beginning of the gouging region, although this is only a coarse approximation. The true shape of the pressure function is not well known; however it still decreases with distance towards the rear of the gouging region. The other three curves represent combined normalized hydrostatic and capillary pressures (metal pressure) for three possible situations.

When metal pressure is higher than the arc pressure at all times, there is no gouging region. If a fluctuation created one, the forces in the metal would overcome the arc pressure and close the incipient gouging region.

When the metal pressure crosses the pressure curve twice, there are two points at which the metal and arc forces are in

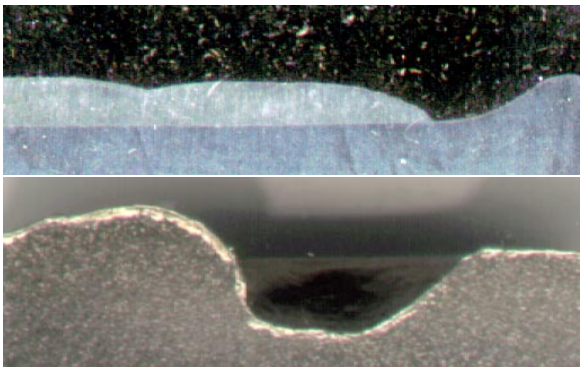

Figure 10: Contact angle for low and high sulfur in AISI 304. The sulfur content of the base metal is 6 ppm for the picture on top, and 230 ppm for that on the bottom. It can be observed that the trailing region with higher sulfur content has a smaller wetting contact angle at the end of the gouging region.

equilibrium. One of these points (point U) is unstable, because any fluctuation which increases the size of the gouging region will increase the relative force of the arc, expanding the gouging region even further, until it reaches the stable point. A fluctuation that decreases the size of the gouging region will create a force balance favorable to the metal pressure, closing the gouging region. At the stable point (point S), a fluctuation that increases the gouging region also increases the closing forces (metal pressure minus arc pressure), and a fluctuation that tends to decrease the gouging region increases the opening forces (arc pressure minus metal pressure).

The third possible case is when the metal pressure crosses the arc pressure curve only once. The crossing point is unstable, and the arc pressure is always larger than the metal pressure. The arc force pushes the transition line ever further, and the trailing end of the weld pool breaks into two parallel streams.

Increases in welding current with a constant metallostatic head, decrease the metal pressure curve by approximately a constant factor (only P_{max} is significantly affected). Increases in the metallostatic head shifts the metal pressure curve upward in a parallel way (only H is significantly affected). When the metal pressure decreases, the transition point moves towards the rear, therefore an increase in current or a decrease in metallostatic head will expand the gouging region.

Example

Figure 12 shows both members of equation 10 with the data from Savage *et al.* [4] (Figure 5), and estimating $r_1 = 1$, $r_2 = 1$, σ=1.3 N/m, and ρ=7000 kg/m^3. These curves correspond to the arc and metal forces at the onset of humping.

The metal pressure curves intersect the arc force curve at about the same point ($x \approx 1.25$), suggesting that the onset of humping occurs when the stable position of the transition line reaches the distance of influence of the arc (x=1).

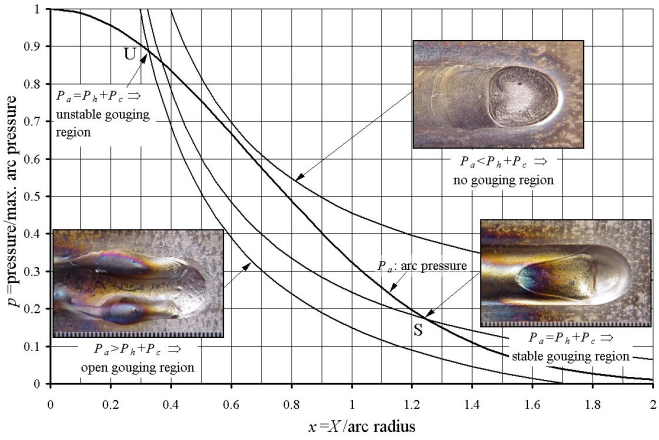

Figure 11: Stability of the gouging region. The bell-shaped curve represents the arc pressure. The other three curves represent the combination of hydrostatic and capillary forces at the transition point. The top curve corresponds to the case when the hydrostatic and capillary forces are larger than the arc pressure, therefore there is no gouging region. The intermediate curve intersects the arc pressure at two points, U (unstable equilibrium), and S (stable equilibrium). Point S determines the extension of the gouging region. If the gouging region extends beyond point S, the hydrostatic and capillary forces become stronger than the arc pressure, decreasing the size of the gouging region. The bottom curve intersects the arc pressure point at an unstable point, and for larger distances the arc pressure dominates over the hydrostatic and capillary forces. The gouging region in this case is open, generating a split bead

Discussion

The good agreement between the proposed humping mechanism, and the experimental data from Figure 12 is encouraging; however, many important factors in the calculation needed to be estimated. For more accurate understanding, a better description of the arc behavior on very deformed weld pools is necessary. The prediction of the onset of humping and the process envelope could be more general if the metallostatic head could be calculated instead of being considered and input of the problem.

A calculation of the curvatures of the free surface would also increase accuracy, especially if the effect of the contact angle could be stated explicitly. The sulfur content of the material affects the contact angle of the trailing region, thus determining the presence or absence of humping in some critical cases (low sulfur helps prevent humping).

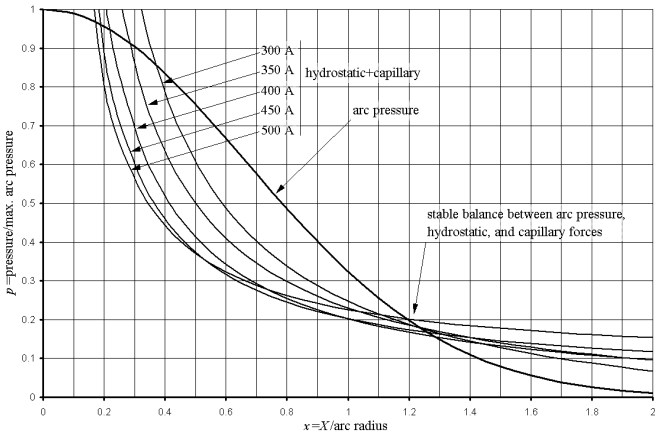

Figure 12: Force balance at the transition point at the onset of humping. These curves have been calculated using equation 10 and the experimental data by Savage [4] for weld pool geometry, and Choo [13] for the arc pressure. The extension of the gouging region is determined by the point where the arc pressure, hydrostatic and capillary forces have a stable balance. For a range of currents, and at the onset of humping, the gouging region extends slightly beyond the arc region (x=1.2 to 1.3). This fact supports the idea that in the conditions these welds were made, humping was determined by the freezing of the thin liquid layer that extended beyond the hot region of the arc.

Conclusion and Recommendations

The high productivity regime is characterized by a very deep weld pool depression (gouging region), where the molten metal under the arc turns into a thin film that flows towards a bulk of liquid (trailing region) at rear of the weld pool. A balance of forces at the transition line between the gouging and trailing regions determine how far towards the rear the gouging region extends. If it extends beyond the region heated by the arc, the thin liquid film will freeze at that point generating a defect such as humping or a split bead. The location of the transition line relative to the size of the region heated by the arc can be estimated using equation 10.

Productivity can be enhanced by using the forehand technique. In this technique the welding torch is tilted in such a way that the plasma jet has a velocity component in the direction of motion of the torch. The main effect of this is to lower the arc pressure that is pushing the transition point into the cold region. This beneficial effect of the forehand technique was observed by Bradstreet [1] and Shimada [3].

If the workpiece was inclined so that the welding direction is downward, it is reasonable to expect that gravity forces (which push the transition point towards the hot region) would become more important, and the welding speed limit would be increased. Additional experiments would be necessary to test this hypothesis, since no studies about such a technique have been reported in the welding literature.

Another possibility for improving welding productivity would be to modify the arc behavior, such that the arc pressure at the transition point decreases, but the hot region remains approximately the same. More knowledge of the welding arc is necessary for effectively implementing this. It is known, however, that blunt GTAW electrodes generate less pressure than sharp ones at the same currents [14, 15]; therefore, the welding speed limit of the former should be higher than of the latter. This effect was experimentally observed by Savage [4]. A method for improving productivity by modifying the arc with magnetic fields was proposed by Grigorenko *et al.* [16]. The use of a different shielding gas could also reduce the arc pressure.

Stainless steel with lower sulfur was found to have a welding speed limit greater than that with high sulfur. Switching to low sulfur steels (of the order of 6 ppm) could dramatically improve the welding conditions. One important difference observed in the welding of steels with different amounts of sulfur is that the "contact angle" of the trailing region was more "non-wetting" for high sulfur than for low sulfur. This affects the capillary forces shifting the balance towards larger gouging regions, thus generating humping. The effect of additives in the metal or in the shielding gas aiming at correcting this defect is an unexplored area that could yield important results.

Acknowledgement

This work was supported by the United states Department of Energy, Office of Basic Energy Sciences.

References

[1] B. J. Bradstreet. *Weld. J.*, pages 314s–322s, (July 1968).

[2] T. Yamamoto and W. Shimada. In *International Symposium in Welding*, Osaka, Japan, (1975).

[3] W. Shimada and S. Hoshinouchi. *Quart. J. Japan Weld. Soc.*, 51(3):280–286, (1982).

[4] W. F. Savage, E. F. Nippes, and K. Agusa. *Weld. J.*, pages 212s–224s, (July 1979).

[5] F. Gao and A. A. Sonin. *Proc. R. Soc. Lond. A*, 444:533–554, (1994).

[6] U. Gratzke, P. D. Kapadia, J. Dowden, J. Kroos, and G. Simon. *J. Phys. D: Appl. Phys.*, 25:1640–1647, (1992).

[7] K. C. Mills and B. J. Keene. *Int. Materials Rev.*, 35(4):185–216, (1990).

[8] K. Ishizaki. In *Physics of the Welding Arc*, pages 195–209, London, UK, (1962). The Institute of Welding.

[9] P. F. Mendez and T. W. Eagar. In *Trends in Welding Research*, pages 13–18, Pine Mountain, GA, (1998). ASM International.

[10] Y. Adonyi, R. W. Richardson, and W. A. Baeslack III. *Weld. J.*, pages 321s–330s, (September 1992).

[11] R. T. C. Choo. *Mathematical Modelling of Heat and Fluid Flow Phenomena in a Mutually Coupled Welding Arc and Weld Pool*. Doctor of Science, Massachusetts Institute of Technology, (1991).

[12] M. L. Lin and T. W. Eagar. *Weld. J.*, pages 163s–169s, (June 1985).

[13] R. T. C. Choo, J. Szekely, and R. C. Westhoff. *Weld. J.*, 69(9):346s–361s, (1990).

[14] R. A. Chihoski. *Weld. J.*, pages 210–222s, (May 1968).

[15] S.-Y. Lee and S.-J. Na. *Weld. J.*, pages 269s–279s, (September 1996).

[16] V. V. Grigorenko, O. N. Kiselev, G. G. Chernyshov, E. A. Gladkov, A. M. Rybachuk, Y. N. Bobylev, N. V. Zhulidov, and G. G. Poklonov. 11(1):58–60, (1997).